An environmentally benign antimicrobial nanoparticle based on a silver-infused lignin core

Alexander P. Richter[1], Joseph S. Brown[1], Bhuvnesh Bharti[1], Amy Wang[2], Sumit Gangwal[2], Keith Houck[2], Elaine A. Cohen Hubal[2], Vesselin N. Paunov[3], Simeon D. Stoyanov[4,5], and Orlin D. Velev[1*]

[1] *Department of Chemical and Biomolecular Engineering North Carolina State University, Raleigh, NC 27695, USA*

[2] *United States Environmental Protection Agency, Office of Research and Development, RTP, NC 27711, USA*

[3] *Surfactant and Colloid Group, Department of Chemistry, University of Hull, Hull, HU67RX, UK*

[4] *Laboratory of Physical Chemistry and Colloid Science, Wageningen University, Wageningen, The Netherlands*

[5] *Department of Mechanical Engineering, University College London, Torrington Place, London, WC1E 7JE, UK*

* *Correspondence to: odvelev@ncsu.edu*

Silver nanoparticles have antibacterial properties, but their use has been a cause for concern because they persist in the environment. Here, we show that lignin nanoparticles infused with silver ions and coated with a cationic polyelectrolyte layer form a biodegradable and green alternative to silver nanoparticles. The polyelectrolyte layer promotes the adhesion of the particles to bacterial cell membranes and, together with silver ions, can kill a broad spectrum of bacteria, including *Escherichia coli*, *Pseudomonas aeruginosa* and quaternary-amine-resistant *Ralstonia sp*. Ion depletion studies have shown that the bioactivity of these nanoparticles is time-limited because of the desorption of silver ions. High-throughput bioactivity screening did not reveal increased toxicity of the particles when compared to an equivalent mass of metallic silver nanoparticles or silver nitrate solution. Our results demonstrate that the application of green chemistry principles may allow the synthesis of nanoparticles with biodegradable cores that have higher antimicrobial activity and smaller environmental impact than metallic silver nanoparticles.

Silver nanoparticles (AgNPs) possess broad-spectrum antimicrobial, antifungal[1] and antiviral[2] activity. They are shown to be effective in killing prokaryotic microorganisms like *Escherichia coli (E.coli)*[3], *Pseudomonas aeruginosa (P. aeruginosa)*[4], and antibiotic-resistant bacterial strains[5]. AgNPs are believed to interfere with essential bacterial cell functions upon contact[6], although the exact mechanism of the antimicrobial effect is still subject to debate[7]. However, after their intended use, the waste nanoparticles are hard to recover or deactivate in solid-waste incineration plants[8] or wastewater treatment systems[9]. While processes such as sulfidation may over time convert the AgNPs to less hazardous form[10], the long exposure of their core in the environment[11,12] and prolonged activity after their intended application[13] may adversely affect multiple ecosystems[14,15]. For this reason, AgNPs have been recognized as potential environmental hazard[16], and their use is beginning to be regulated in many countries[17,18].

The problems mentioned above can be mitigated by using green chemistry principles[19] at the stage of nanoparticle design. So far, these principles have been applied to AgNP synthesis[20,21] by using safer solvents and auxiliaries[22], which , however, does not solve the problem of persistent nanoparticle waste. We demonstrate that an environmentally-friendly solvent synthesis can be combined with other green chemistry principles to make a class of sustainable nanoparticles with short term activity as substitutes for antimicrobial metallic AgNPs. Since the antimicrobial action of AgNPs stems from the localized emission of Ag^+ ions at the microbes' cell walls[23], we envisaged that it is not necessary for the whole nanoparticle to be made of silver, as its metallic core would remain unused and may eventually be released in the environment. Instead, we replaced the AgNPs with cores of degradable common biopolymer, which can be easily precipitated into nanoparticles of desired size by using environmentally-friendly solvents. The degradable cores are infused with minimal amount of Ag^+ ions needed for bactericidal action and are surface-functionalized to increase affinity towards targeted (bio)substrates. Such nanoparticles would rapidly lose their post-utilization activity and biodegrade in the environment after disposal (Fig. 1).

The design of antimicrobial nanoparticles requires understanding of their interactions with the intended target (microbe) to enhance silver ion antimicrobial efficiency as a way to reduce active material loading. Nanoparticle interactions with living organisms are complex[24] and subject to intensive ongoing research[25]. While the potency of AgNPs depends on a number of nanoparticle-specific[26,27] and bacteria-specific properties[28], their surface charge is likely to be the primary facilitator of their antimicrobial action[29]. Cationic AgNPs are electrostatically attracted to negatively-charged bacterial cell membranes. Their adhesion to the cell surface increases the local silver ion concentration[10]. The Ag^+ ions released at the cell walls may disrupt their membrane integrity[30] and can affect the cells through multiple mechanisms, ultimately leading to their death[31,32]. In order to enhance the adhesion of these silver ion nano-carriers to the microbial cell surface, we coated the silver-infused nanoparticle cores with a layer of cationic

polyelectrolyte. The results demonstrate that such engineered nanoparticles could be as efficient as their AgNPs analogs, but have time-limited antimicrobial activity because of depletion of the bioactive Ag^+ ions.

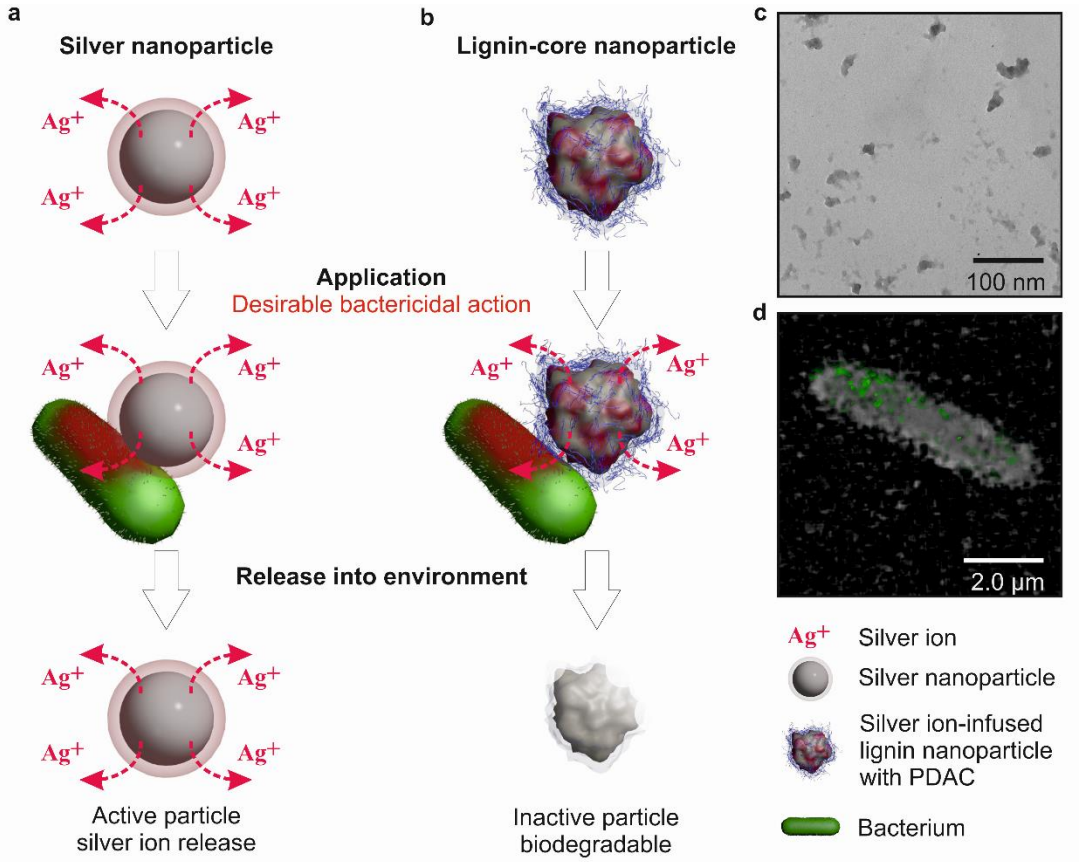

Figure 1 | Schematics of the general use cycle and principle of bactericidal action of the environmentally-benign lignin-core nanoparticles (EbNPs) compared to the presently used silver nanoparticles (AgNPs). a, General mechanism of antimicrobial action of common AgNPs via release of Ag^+ ions, which continues post utilization. **b,** Antimicrobial action mechanism of Ag^+ ion-infused EbNPs with cationic polyelectrolyte coating, which facilitates electrostatic attraction between the EbNPs and the negatively charged cell walls. In contrast to AgNPs, EbNPs are depleted of silver ions during application, minimizing their post-utilization activity. **c,** TEM micrograph of as-synthesized EbNPs in the size range of 40 to 70 nm. **d,** Confocal microscopy image of EbNPs with polyelectrolyte coating adhering to the cell membrane of *E. coli*.

Fabrication and characterization of EbNPs

We choose lignin, one of the most abundant and underutilized biopolymers in nature[33], as a benign particle core material. The used lignin was Indulin AT, which is extracted from biomass as by-product of the Kraft pulping processes[34]. It is soluble in alkali solutions, but insoluble in neutral and acid conditions and has high absorbance capacity for heavy metal ions in environmental remediation processes[35,36]. We showed earlier how biopolymer micro- and nanoparticles can be synthesized via an entirely water-based, solvent free, pH-drop flash precipitation method[37,38]. A similar pH-drop flash precipitation in ethylene glycol

solution can be applied to synthesize negatively-charged pH-stable Indulin AT lignin nanoparticles of controlled sizes[38]. The nanoparticles could be synthesized in a broad size range (Fig. 2a); the ones used as EbNP precursors after dialysis had a mean hydrodynamic diameter of 84 ± 5 nm as measured by Dynamic Light Scattering and a zeta potential of -33 ± 1 mV (see supplementary information (SI) for measurement details).

In the next step, the lignin nanoparticle cores were infused with Ag^+ ions at pH 5.0 by using an aqueous solution of $AgNO_3$ as silver source. The IAT lignin has several functional groups, e.g. carboxylic, thiol, phenolic and aliphatic hydroxyl groups (see Table S1 in SI) that can serve as binding sites for silver ions[35,36]. Previous studies indicated that the particles are porous[38,39], which would increase the total available surface area for silver ion loading and could potentially increase their degradation rate in the environment after disposal[38]. The interaction of Ag^+ ions with the particles was investigated by characterizing the adsorption equilibria (Fig. 2b, see also Fig. S1 and Table S2 in SI) and the Ag^+ desorption kinetics (Fig. 2c). These data taken together indicate the presence of high and low energy binding sites, as not all adsorbed Ag^+ ions are released after 48h (Fig. 2c). The net binding of Ag^+ ions onto the EbNPs could be modeled on the basis of a modified Langmuir adsorption isotherm $\Gamma(c) = \Gamma_{\max} K\, c\,/(1 + K\, c) + \Gamma_1$, where Γ and c are the respective surface and bulk equilibrium concentrations of silver ions; $\Gamma_{\max}$ is the maximum surface loading for weakly bound silver ions, K is the adsorption constant, which relates to the Ag^+ binding energy to the particles[40], and Γ_1 is the adsorption of strongly bound silver ions in the high affinity region in mg/g of EbNPs. The least square fitting of the experimental data in Fig. 2b at value of Γ_1 = 1.4 Ag^+ per gram obtained from desorption data (see below) resulted in $\Gamma_{\max}$ = 9.17 Ag^+ mg/g and K = 0.11 L/mg Ag^+ (see Table S3 in SI for details).

The Ag^+ release profile of nanoparticles infused with 4.9 Ag^+ mg/g in pure water is plotted in Figure 2c (see Table S4 in SI for Ag^+ ion adsorption measurements). The silver ions adsorbed in the high affinity region (≈ 35% of the initial concentration) may not be released readily. However the weakly bound Ag^+ ions adsorbed in the low affinity region are released during application. The release data can be fitted with exponential decay curve, offset by the strongly bound silver ions in the high affinity region (Fig. 2c), $\Gamma(t) = \Gamma_1 + \Gamma_0\, e^{-t/\tau}$, where Γ_0 is the weakly bound silver load, t is the time and τ the characteristic decay time. The least square fit resulted in values of Γ_1 = 1.4 Ag^+ mg/g and τ = 6.2 h (see Table S3 in SI for fitting details). In summary, the data indicate that more than 95 % of the silver ions in the low affinity region are released within the first 24 h, which is consistent with their anticipated application time.

After silver ion infusion, EbNPs-Ag^+ are electrostatically stabilized and have a negative zeta-potential of -32 mV ± 1 mV (see SI for measurement details). In the last step, the surface charge of the particles was reversed by the adsorption of a cationic polyelectrolyte, polydiallyldimethylammonium chloride (PDAC), which may also delay slightly the release of silver ions from the particles (Fig. S2 in SI) due to formation

of electrostatic barrier for their release. Stable EbNPs 0.05 wt% with positive surface potential could be fabricated at weight ratio of PDAC/Indulin AT of 0.20 or higher as shown in Fig. 2d. The TEM image in Fig. 1c displays nanosized non-spherical clusters with sizes below 70 nm. The accumulation of these cationic EbNPs on negatively charged *E.coli* was visualized by confocal microscopy (Fig. 1d). The ionic silver in these PDAC-coated, Ag^+-loaded EbNPs (EbNPs-Ag^+-PDAC) could be readily released via desorption near the cell walls, which could explain their strong antimicrobial efficacy reported below.

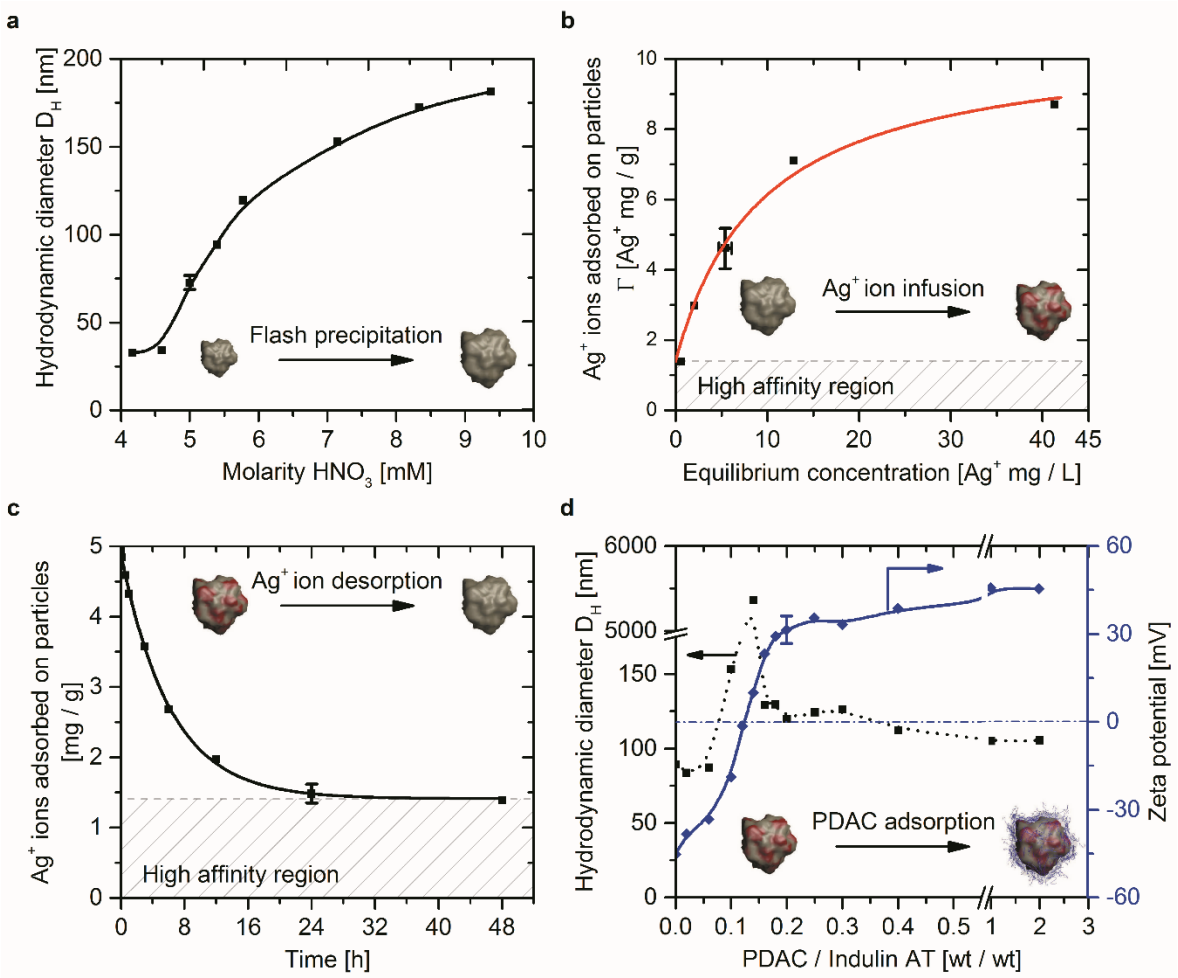

Figure 2 | Synthesis and characterization of environmentally-benign nanoparticles. a, Size control - diameter of EbNPs as a function of HNO_3 added during the flash precipitation. The diameter of EbNPs increases with addition of larger amounts of HNO_3. **b,** Amount of Ag^+ ions adsorbed on the EbNPs as a function of equilibrium silver ion concentration. The data are fitted on basis of a modified Langmuir adsorption isotherm (see text). **c,** Amount of Ag^+ ions retaining in the EbNPs in silver ion depletion test as a function of time (initial load of 3.5 Ag^+ mg/g). The particles release more than 95 % of the weakly bound Ag^+ within the first 24 h. **d,** Surface charge modification - diameter and zeta potential of EbNPs as a function of PDAC added. PDAC / Indulin AT weight ratios between 0.10 and 0.15 result in aggregation of EbNPs. PDAC to Indulin AT wt% ratios of 0.20 or higher result in stable suspensions of PDAC-

coated EbNPs with positive surface charge. Error bars represent the standard deviation of corresponding experimental values.

Antimicrobial activity of EbNPs

The antimicrobial activity of EbNPs-Ag^+-PDAC nanoparticles was evaluated within 6 h after their preparation. Quantitative antimicrobial tests were performed on gram-negative *E. coli BL21(DE3)*, a common testing bacteria related to pathogenic *E.coli* such as O157:H7, which has been genetically modified not to secrete toxin, and *P. aeruginosa* (ATCC 15442), a highly adaptive pathogen used in standardized disinfectant testing in the food industry[41]. Antimicrobial testing on a quaternary amine-resistant *Ralstonia sp.* was also performed to distinguish the antimicrobial effect of Ag^+ ions from PDAC controls, and to evaluate the post-utilization activity of silver-depleted EbNPs. Finally, qualitative antimicrobial tests were performed on *Staphylococcus epidermidis (S. epidermidis), strain PCI 1200* (ATCC 12228) to evaluate the activity of the particles towards gram-positive bacteria. The testing was carried out according to a standardized exposure protocol (Fig. S3) at three contact times, 1 min, 30 min and 24 h. The activity of each sample was determined by counting the colony-forming units (CFU) and comparing the CFUs on test and reference plates (Fig. S4). The maximal antimicrobial reduction efficiency of 100% was reached when no CFUs were detectable on the test plate. The EbNPs efficiency was compared against positively charged branched polyethyleneimine-coated AgNPs (BPEI-AgNPs) and $AgNO_3$ solutions. BPEI-AgNPs have a surface charge similar to the functionalized EbNPs and are known for their excellent antimicrobial activity compared to other common AgNPs[29,42]. The BPEI-AgNPs were synthesized via photoreduction of $AgNO_3$ solution[43] and had a hydrodynamic diameter of 20 ± 10 nm. Six different samples of BPEI-AgNPs and $AgNO_3$ solutions with Ag^+ ion equivalent concentrations ranging from 5 to 100 Ag^+ mg/L (ppm) were investigated.

The CFU reduction efficiencies of the samples in *E. coli* tests are compared as a function of the silver content by mass in Fig. 3a and 3b (see also Fig. S5 and Table S5 in SI). The EbNPs-Ag^+-PDAC exhibited strong antimicrobial activity after 1 min exposure, while the corresponding nanoparticle-free supernatant showed no observable effect. The supernatant showed some CFU reduction after 30 minutes, which can be explained by residual amounts of unbound PDAC or silver. The conventional BPEI-AgNPs and $AgNO_3$ solutions were less effective after 1 min, but after 30 min contact time reached 100% microbicidal efficiency at 50 mg/L Ag^+ equivalent. EbNPs-Ag^+ without PDAC coating did not result in significant CFU reduction (5%), which may be attributed to their negative surface charge reducing the particle adhesion to the bacteria. However, EbNPs-PDAC without silver also showed strong CFU growth suppression, which may be attributed to the antimicrobial effect of the quaternary amine coating (note also that PDAC control reached 100% bacteria reduction after 30 min).

The antimicrobial efficiencies data on *P. aeruginosa* after 30 min are compared in Fig. 3c. The EbNPs-Ag^+-PDAC sample resulted in strong CFU reduction at 5 mg/L Ag^+ equivalent (this sample reached 100% reduction after 24 h, see Fig. S6 in SI). Interestingly, BPEI-AgNPs did not exhibit observable antimicrobial activity even at 100 mg/L Ag^+ equivalent. $AgNO_3$ solutions were inactive up to 40 mg/L Ag^+ equivalent and exhibited low CFU reduction at 60 mg/L Ag^+. The control PDAC solutions at 0.02 wt% did not exhibit observable CFU reduction after 30 min contact time, and the PDAC solutions at 0.04 wt%, double the amount used in EbNPs-Ag^+-PDAC sample, exhibited strong CFU reduction. However, again the EbNPs-Ag^+-PDAC performed best in terms of antimicrobial efficiency, demonstrating higher efficiency than $AgNO_3$ solution containing 12× more Ag^+, and BPEI-AgNPs containing 20× higher Ag equivalent. These EbNPs were also 100% effective against the gram-positive bacteria *S. epidermidis* (see Table S7 in SI).

The CFU reduction data on PDAC-resistant *Ralstonia sp.* after 30 min contact time are compared in Fig. 3d. The EbNPs-Ag^+-PDAC, $AgNO_3$ solutions, and BPEI-AgNPs all resulted in 99%+ CFU reduction at ≥ 5 mg/L Ag^+ equivalent. The EbNPs-Ag^+ without PDAC coating reached moderate CFU reduction at 10 mg/L Ag^+ after 30 minutes. PDAC solution at 0.04 wt% did not show any CFU reduction even after 24 h of contact (see Fig. S7 and Table S6 in SI). Similarly, lignin-only EbNP controls did not result in any observable CFU reduction in all tests; on the contrary, they promoted CFU growth to some extent (see Fig. S8 in SI).

In summary, comparing all active agents tested in terms of broad-spectrum antimicrobial efficiency, we establish that EbNPs-Ag^+-PDAC proved most effective against four types of gram-positive and gram-negative bacteria. These EbNP particles also outperformed the common AgNPs and $AgNO_3$ solutions on *E. coli* and *P. aeruginosa* while using at least 10× lower Ag^+ equivalent concentrations. The EbNPs-Ag^+-PDAC also outperformed PDAC on *Ralstonia sp.* The high activity of EbNPs-Ag^+-PDAC likely stems from the combination of the antimicrobial properties of Ag^+ ions and the PDAC coating, especially on cells that are sensitive to quaternary amines. However, for bacteria resistant to charged amines, such as the *Ralstonia sp.*, the effect of EbNPs-Ag^+-PDAC is a direct result of the bactericidal activity of silver ions.

Finally, the post-utilization activity of EbNPs-Ag^+-PDAC depleted from silver ions was evaluated on PDAC-resistant *Ralstonia sp*. We simulated the post-application depletion process of silver from EbNPs-Ag^+-PDAC, which were originally infused with 5 mg/L Ag^+ ions, by dialysis in DI water for 24 h. This led to silver ion desorption similar to the one that would occur if the particles were disposed in environmental water. The residual silver ion content in these dialyzed samples was determined to be 0.89 mg/L Ag^+ ions using Inductively-Coupled Plasma Optical Emission Spectroscopy (ICP-OES), which translates to 18 % of Ag^+ remaining bound on the particles and is in good correspondence with the release kinetics studies described above. The silver-depleted EbNPs-Ag^+-PDAC sample exhibited moderate CFU reduction of 66 % on *Ralstonia sp*. at 24 h contact time, but showed bacterial film formation due to excessive cell

multiplication at 96 h, while the non-silver-depleted EbNPs-Ag^+-PDAC control had 100% CFU reduction at 24 h (see Fig. S8 in SI). This result indicates that EbNPs-Ag^+-PDAC nanoparticles would lose their antimicrobial activity due to Ag^+ ion depletion when exposed to the environment. The lignin cores depleted from silver ions would in turn be further degraded by the microbial flora present in the environment.

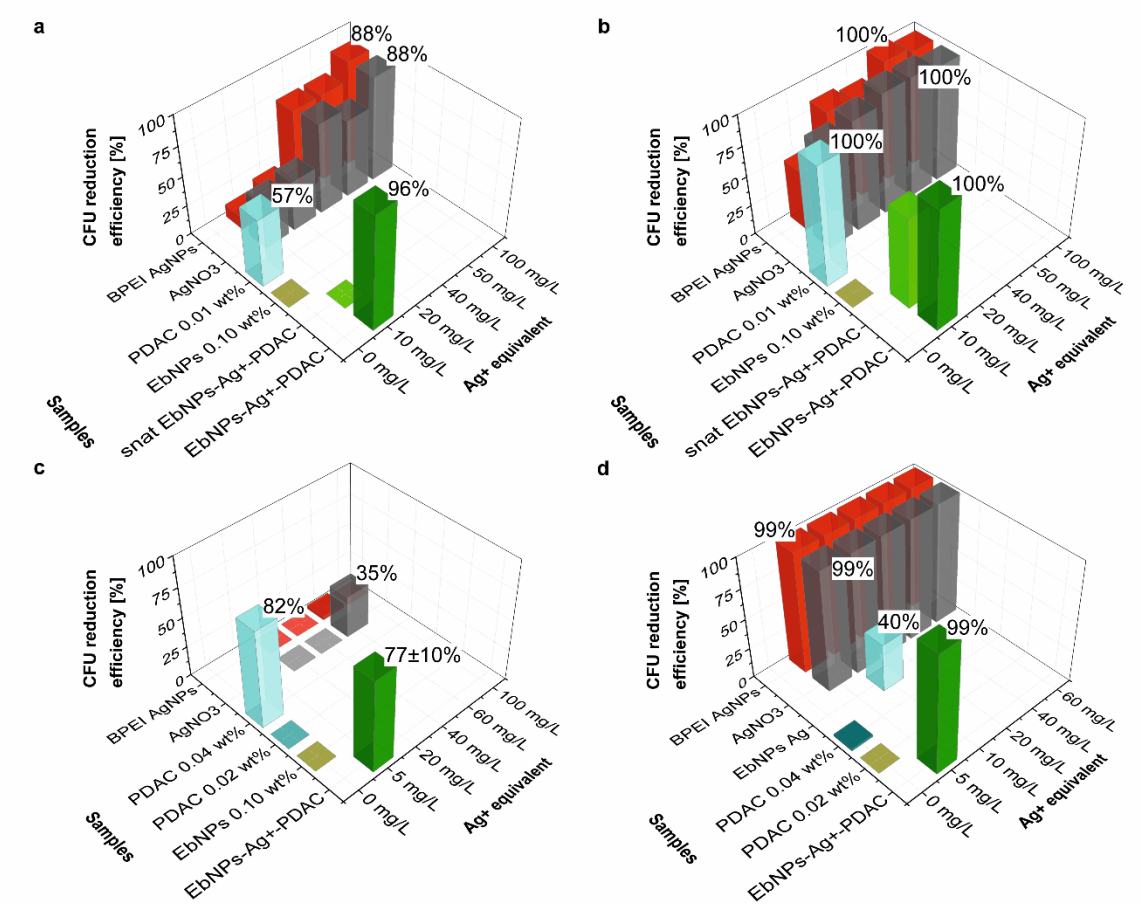

Figure 3 | Q**uantification of Colony Forming Unit reduction efficiency as a function of mg/L Ag^+ equivalent of EbNPs and control samples on *E. coli, P. aeruginosa*, and *Ralstonia sp*. a,** *E. coli* test – 1 min contact time. The fully functionalized sample is EbNPs-Ag^+-PDAC. It is compared to a number of controls, including the centrifuged supernatant solution from the sample ("snat"), EbNPs without Ag^+, PDAC polyelectrolyte solution, $AgNO_3$ solution and BPEI-coated AgNPs. EbNPs-Ag^+-PDAC achieved the highest CFU reduction of all samples with the smallest amount of silver. **b,** *E. coli* test – 30 min contact time. Note that in addition to silver ion-releasing EbNPs and AgNPs, the cationic polyelectrolyte PDAC is highly efficient. **c,** *P. aeruginosa* test – 30 min contact time. EbNPs-Ag^+-PDAC and PDAC turn out to be much more efficient than common AgNPs and $AgNO_3$ solution. **d,** PDAC-resistant *Ralstonia* test – 30 min contact time. For these bacteria EbNPs-Ag^+-PDAC, BPEI-AgNPs and $AgNO_3$ solutions outperformed PDAC samples. Note that EbNPs-Ag^+-PDAC is the only sample that is consistently efficient at very low Ag^+ loading. The experiments were performed three times, and the error bars represent the range of average values.

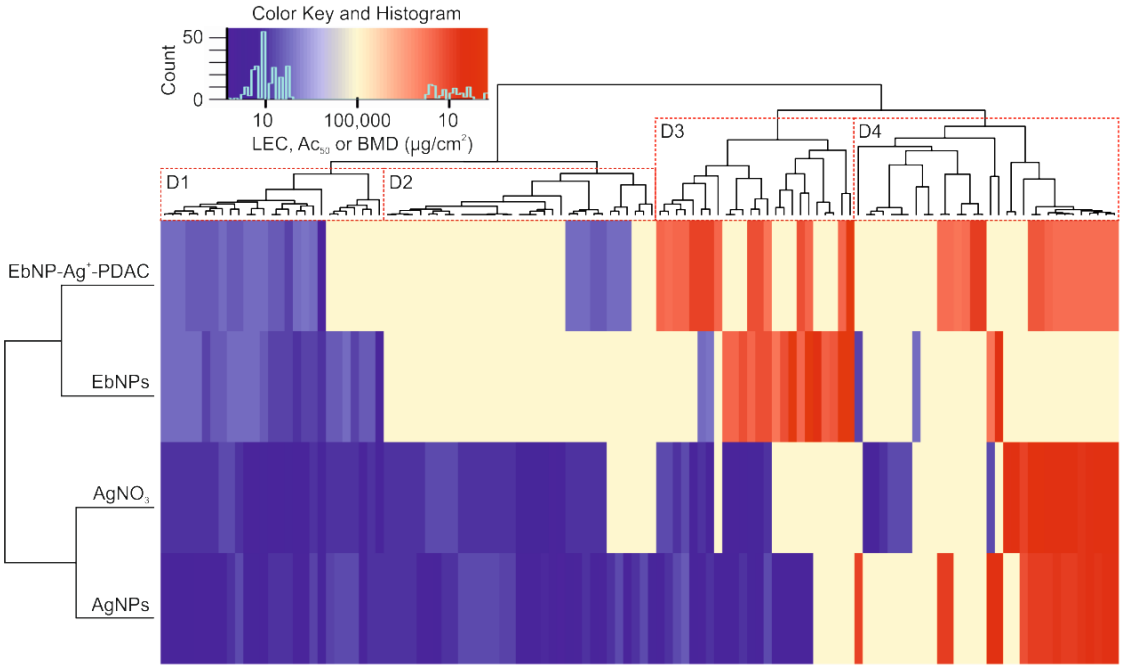

Figure 4 | Heat map of the bioactivity of EbNPs-Ag$^+$-PDAC, EbNPs, $AgNO_3$ (aq) and AgNPs, based on ToxCast mammalian cell and zebrafish embryo screening assays. The heat map reports on activities in assays (see Fig. S11 in SI for detailed assay labeling) at either the Lowest Effective Concentration (LEC), concentration at 50% of maximum activity (AC_{50}), or Benchmark Dose (BMD). The color coding relates to the sample mass concentrations where significant changes are registered as follows: blue and red colors both indicate measureable deviations in the assays from neutral activities, which are shown in yellow and arbitrarily set on 100,000. Deeper red indicate increases starting at lower concentrations than light red, deeper blue indicate decreases starting at lower concentrations than light blue. The heat-map shows that based on total sample mass concentrations, AgNPs and $AgNO_3$(aq) had very similar profiles, and affected more assays (blue and red) than EbNPs and EbNPs-Ag$^+$-PDAC.

High-throughput screening of EbNPs bioactivity

The biological activity and potential toxicity hazards of the particles were investigated in a comprehensive testing by the U.S. EPA's ToxCast program[44] protocols as described in the Methods. The 156 biological endpoints are described in the Methods. The aggregate assay targets are divided into ten biological function groups (see Fig. S9 in SI), namely zebrafish development toxicity, acute inflammation, cell cytotoxicity, cell proliferation, cellular stress modulation, immune response, nuclear receptor activation, tissue remodeling modulation, and vascular biology modulation. The testing results are summarized in the bioactivity "heat map" in Fig. 4. The data indicate that EbNPs and EbNPs-Ag$^+$-PDAC had response profiles more similar to each other than to AgNP or $AgNO_3$(aq). When evaluated on a total mass basis at Lowest Effective Concentration (LEC) > 0.1 µg/mL, they also affected fewer biological endpoints in all biological functional groups than AgNPs or $AgNO_3$ (aq) (see Fig. S9 in SI). At LEC < 0.1 µg/mL the results show the

same trend, although some endpoints (e.g. in immune response) were affected at lower Ag^+ ion concentration by EbNPs-Ag^+-PDAC than by AgNPs. When evaluated by equivalent silver ion concentration, EbNPs-Ag^+-PDAC appeared to affect zebrafish embryos at lower silver content than AgNPs (see Fig. S10 in SI).

Overall, the bioactivity screening results show that the lignin-only EbNPs without Ag^+ loading and the EbNPs-Ag^+-PDAC interfered with fewer biological pathways than the $AgNO_3$(aq) and AgNPs. Thus, it could be expected that the EbNPs-Ag^+-PDAC would also have a much smaller environmental impact in terms of amount of silver released, as they would contain much less silver by mass than the common AgNPs in antimicrobial application scenarios relating to higher silver "atom economy"[19]. Their impact is likely to be minimized further as the EbNPs, unlike the persistent AgNPs, can rapidly lose their activity due to Ag^+ ion depletion in the environment or wastewater, followed by natural pathways for the neutralization of the minimal amount of ionic silver[45]. The EbNPs surface modifier, PDAC, commonly used as a primary organic coagulant in waste water treatment[46], is also likely to be readily neutralized once it interacts with naturally occurring biopolymers[47]. The lignin NPs depleted of Ag^+ and PDAC would biodegrade similarly to lignin from plant biomass[48,49]. The EbNPs are also likely be more readily degraded and removed than common AgNPs in waste water treatment systems or in waste incineration plants.

Conclusions

We report a class of antimicrobial nanoparticles with biodegradable cores (from Indulin AT lignin), loaded with Ag^+ ions and coated with cationic polyelectrolyte PDAC. The EbNPs-Ag^+-PDAC exhibit broad spectrum biocide action and are capable of neutralizing common gram-negative and gram-positive human pathogens as well as quaternary amine-resistant bacteria, while using 10× less silver when compared with conventional BPEI-AgNPs and $AgNO_3$ aqueous solution. The PDAC coating, which boosts their adhesion to microbial cell membranes, may have some antibacterial activity on its own; however, both EbNP controls without PDAC or without Ag^+ ion loading demonstrated much lower antimicrobial efficiencies, indicating that both agents act synergistically. The array of high-throughput screening tests on mammalian cells and zebrafish embryos indicate that the EbNPs have decreased impact on the majority of biological endpoints, when compared with AgNPs and $AgNO_3$ by total mass. In addition, the EbNPs-Ag^+-PDAC showed time-limited antimicrobial action since they can lose their residual silver ions by post-utilization dilution in water. We expect that the overall environmental impact of EbNPs-Ag^+-PDAC is likely to be significantly lower when compared to AgNPs, however, more research and long-term testing in realistic real-world conditions (such as in water containing salts, surfactants and pollutants) would be needed to fully validate these claims. In more general plan, these environmentally-benign nanoengineering results illustrate how green chemistry

principles including atom economy, use of renewable feedstocks, and design for degradation can be applied to design more sustainable nanomaterials with increased activity and decreased environmental footprint.

Methods

Synthesis of Ag^+-infused Indulin AT nanoparticles with PDAC coating. Native Indulin AT lignin nanoparticles were synthesized in ethylene glycol similarly to the method described earlier[38] and detailed in the SI. The native Indulin AT nanoparticles were subsequently functionalized with silver ions from $AgNO_3$ in aqueous solution. The Ag^+-infused EbNPs were coated with PDAC by rapidly mixing 1:1 by volume of EbNP suspension with PDAC solution.

Cell culture and microbial testing. *E. coli BL21(DE3), P. aeruginosa (ATCC 15442),* and *S. epidermidis* (ATCC 12228) bacteria were grown in nutrient broth. The subsequent dilution series was performed with nutrient broth and the bacteria were stored at 4°C before exposure to active agents. PDAC resistant *Ralstonia sp.* were stored in freshly prepared PDAC 0.02 wt% solutions (for bacteria isolation and analysis see SI). $AgNO_3$ testing solutions were prepared from a 1000 mg/L Ag^+ reference standard. The target concentrations of Ag^+ in mg/L for antimicrobial testing were reached by diluting the reference standard with Millipore water. The schematics in Fig. S3 in SI describe the protocol for antimicrobial testing. 200 µL of each active agent was placed into separate low retention centrifuge tubes. 100 µL of PBS buffer (in *Ralstonia* test 100 µL of DI water instead of PBS buffer) was added to each tube to baseline the ionic strength, and to adjust the pH value to 7. Finally, 100 µL of bacteria, *Ecoli* or *P. aeruginosa*, suspension with approximately 1000 to 4400 CFU/mL in nutrient broth (*Ralstonia sp.* in PDAC 0.02 wt% solution), was added. The samples were continuously vortexed. After the bacteria were exposed to the active agent for a given time, e.g. 30 minutes, the survival rate of the bacteria was determined by plating 100 µL of each sample evenly distributed on Luria-Bertani agar plates. The procedure was repeated after various exposure time. After the plating procedure, the Petri dishes were sealed and incubated upside down for 48 h at 37 °C.

Depletion of silver-infused EbNPs. The EbNPs-Ag^+ samples for the depletion study were depleted from Ag^+ in 0.5 mL Slide-A-Lyzer MINI Dialysis Devices by dialysis against 13.6 mL Millipore water between 5 min and 48 h. The sample EbNPs-Ag^+-PDAC (20 mL) for bioactivity testing was depleted from Ag^+ using dialysis tubing against 380 mL of DI water for 24 h without exchanging the dialysis water. The equilibrated samples were collected and their silver contents were measured with Inductively Coupled Plasma Mass Spectroscopy (ICP-MS) and Optical Emission Spectroscopy (ICP-OES) (for experimental description see SI).

Biological activity and toxicity hazards tests. EbNPs-Ag^+-PDAC, EbNPs, $AgNO_3$, and AgNPs of 15 nm diameter (ENPRA NM300)[50] were screened for 156 endpoints in five cell-based platforms used in ToxCast, the U.S. EPA's chemical testing and prioritization program[44]. The bioactivity assays used human primary cell (co)culture and cell lines, rat primary hepatocytes, and developing zebrafish embryos with a diverse range of toxicity early responses and

phenotype endpoints. Gold (Au) nanoparticles, included as relatively inert nanomaterial controls, and Ag microparticles affected very few assays (Fig. S9f and S9g in SI), indicating that particles having the feature of being nanosized (AuNP), or containing Ag alone, do not exhibit broad or high bioactivity.

Acknowledgements

The authors acknowledge the funding from U.S. EPA via Pathfinder Innovation Projects grant, US NSF Tringle Center for Programmable Soft Matter (DMR-1121107) and North Carolina State University. We thank D. Plemmons and A. K. Sarkar for assistance in initial studies, and H. Armstrong for assistance in silver ion desorption studies. We are grateful to M. Moore for the analysis and characterization of PDAC-resistant *Ralstonia sp.* bacteria, R. Garcia for TEM analysis and K. Hutchinson and the ASSL at NCSU for silver content analysis. SDS thanks for the financial support of EU COST actions MP1305 and MP1106 as well the EU Project FP7-REGPOT-2011-1, "Beyond Everest".

Author contributions

APR planned and performed the key experiments and analyzed the results. JSB synthesized EbNPs and tested their antimicrobial efficiency. BB contributed with discussions and confocal microscopy imaging. AW, SG, KH, and EAH carried out the EPA toxicity evaluation, analyzed and plotted the ToxCast data. APR, AW and ODV analyzed the results, and all authors discussed them and commented on the manuscript. ODV, VNP and SDS conceived this project and contributed with ideas and analysis. ODV is the principal investigator who led the research team.

Disclaimer

This manuscript has not been endorsed or institutionally approved for publication by the US Environmental Protection Agency.

Competing financial interest

APR, VNP, SDS and ODV declare potential financial interests in the future development and commercialization of similar nanomaterials. NC State University has filed a patent application (PCT/US2014/022382) and has licensed the EbNP technology to a commercial entity.

References:

1 Panáček, A. *et al.* Antifungal activity of silver nanoparticles against Candida spp. *Biomaterials* **30**, 6333-6340 (2009).
2 Lara, H., Garza-Trevino, E., Ixtepan-Turrent, L. & Singh, D. Silver nanoparticles are broad-spectrum bactericidal and virucidal compounds. *J. Nanobiotechnology* **9**, 30 (2011).
3 Sondi, I. & Salopek-Sondi, B. Silver nanoparticles as antimicrobial agent: A case study on E. coli as a model for gram-negative bacteria. *J. Colloid Interface Sci.* **275**, 177-182 (2004).
4 Poole, K., Krebes, K., McNally, C. & Neshat, S. Multiple antibiotic resistance in Pseudomonas aeruginosa: Evidence for involvement of an efflux operon. *J. Bacteriol.* **175**, 7363-7372 (1993).
5 Panáček, A. *et al.* Silver colloid nanoparticles: Synthesis, characterization, and their antibacterial activity. *J. Phys. Chem. B* **110**, 16248-16253 (2006).
6 Morones, J. R. *et al.* The bactericidal effect of silver nanoparticles. *Nanotechnology* **16**, 2346 (2005).
7 Rai, M., Yadav, A. & Gade, A. Silver nanoparticles as a new generation of antimicrobials. *Biotechnol. Adv.* **27**, 76-83 (2009).
8 Walser, T. *et al.* Persistence of engineered nanoparticles in a municipal solid-waste incineration plant. *Nat. Nanotechnol.* **7**, 520-524 (2012).
9 Jeong, E. *et al.* Different susceptibilities of bacterial community to silver nanoparticles in wastewater treatment systems. *J. Environ. Sci. Health., Part A* **49**, 685-693 (2014).
10 Levard, C., Hotze, E. M., Lowry, G. V. & Brown, G. E. Environmental transformations of silver nanoparticles: Impact on stability and toxicity. *Environ. Sci. Technol.* **46**, 6900-6914 (2012).
11 Chinnapongse, S. L., MacCuspie, R. I. & Hackley, V. A. Persistence of singly dispersed silver nanoparticles in natural freshwaters, synthetic seawater, and simulated estuarine waters. *Sci. Total Environ.* **409**, 2443-2450 (2011).
12 Sharma, V. K., Siskova, K. M., Zboril, R. & Gardea-Torresdey, J. L. Organic-coated silver nanoparticles in biological and environmental conditions: Fate, stability and toxicity. *Adv. Colloid Interface Sci.* **204**, 15-34 (2014).
13 Dobias, J. & Bernier-Latmani, R. Silver release from silver nanoparticles in natural waters. *Environ. Sci. Technol.* **47**, 4140-4146 (2013).
14 Stern, S. T. & McNeil, S. E. Nanotechnology safety concerns revisited. *Toxicol. Sci.* **101**, 4-21 (2008).
15 Ahamed, M., AlSalhi, M. S. & Siddiqui, M. K. J. Silver nanoparticle applications and human health. *Clin. Chim. Acta* **411**, 1841-1848 (2010).
16 Fabrega, J., Luoma, S. N., Tyler, C. R., Galloway, T. S. & Lead, J. R. Silver nanoparticles: behaviour and effects in the aquatic environment. *Environ. Int.* **37**, 517-531 (2011).
17 Justo-Hanani, R. & Dayan, T. The role of the state in regulatory policy for nanomaterials risk: Analyzing the expansion of state-centric rulemaking in EU and US chemicals policies. *Res. Policy* **43**, 169-178 (2014).
18 Marchant, G., Sylvester, D. & Abbott, K. Risk management principles for nanotechnology. *Nanoethics* **2**, 43-60 (2008).
19 Anastas, P. & Eghbali, N. Green chemistry: Principles and practice. *Chem. Soc. Rev.* **39**, 301-312 (2010).
20 Sharma, V. K., Yngard, R. A. & Lin, Y. Silver nanoparticles: Green synthesis and their antimicrobial activities. *Adv. Colloid Interface Sci.* **145**, 83-96 (2009).
21 Kumar, A., Vemula, P. K., Ajayan, P. M. & John, G. Silver-nanoparticle-embedded antimicrobial paints based on vegetable oil. *Nat. Mater.* **7**, 236-241 (2008).
22 Raveendran, P., Fu, J. & Wallen, S. L. Completely "green" synthesis and stabilization of metal nanoparticles. *J. Am. Chem. Soc.* **125**, 13940-13941 (2003).
23 Xiu, Z., Zhang, Q., Puppala, H. L., Colvin, V. L. & Alvarez, P. J. J. Negligible particle-specific antibacterial activity of silver nanoparticles. *Nano Lett.* (2012).
24 Nel, A. E. *et al.* Understanding biophysicochemical interactions at the nano-bio interface. *Nat. Mater.* **8**, 543-557 (2009).
25 Ge, C. *et al.* Towards understanding of nanoparticle–protein corona. *Arch. Toxicol.*, 1-21 (2015).
26 Lundqvist, M. *et al.* Nanoparticle size and surface properties determine the protein corona with possible implications for biological impacts. *Proc. Natl. Acad. Sci. U.S.A.* **105**, 14265-14270 (2008).
27 Verma, A. & Stellacci, F. Effect of surface properties on nanoparticle–cell Interactions. *Small* **6**, 12-21 (2010).
28 Monopoli, M. P., Aberg, C., Salvati, A. & Dawson, K. A. Biomolecular coronas provide the biological identity of nanosized materials. *Nat. Nanotechnol.* **7**, 779-786 (2012).

29 El Badawy, A. M. *et al.* Surface charge-dependent toxicity of silver nanoparticles. *Environ. Sci. Technol.* **45**, 283-287 (2010).
30 Sotiriou, G. A. & Pratsinis, S. E. Antibacterial activity of nanosilver ions and particles. *Environ. Sci. Technol.* **44**, 5649-5654 (2010).
31 Feng, Q. L. *et al.* A mechanistic study of the antibacterial effect of silver ions on Escherichia coli and Staphylococcus aureus. *J. Biomed. Mater. Res.* **52**, 662-668 (2000).
32 Matsumura Y., Y. K., Kunisaki S., and Tsuchido T. Mode of bactericidal action of silver zeolite and its comparison with that of silver nitrate. *Appl. Environ. Microbiol.* **69**, 4278-4281 (2003).
33 Norgren, M. & Edlund, H. Lignin: Recent advances and emerging applications. *Curr. Opin. Colloid Interface Sci.* **19**, 409-416 (2014).
34 Duval, A. & Lawoko, M. A review on lignin-based polymeric, micro- and nano-structured materials. *React. Funct. Polym.* **85**, 78-96 (2014).
35 Guo, X., Zhang, S. & Shan, X.-q. Adsorption of metal ions on lignin. *J. Hazard. Mater.* **151**, 134-142 (2008).
36 Harmita, H., Karthikeyan, K. G. & Pan, X. Copper and cadmium sorption onto kraft and organosolv lignins. *Bioresour. Technol.* **100**, 6183-6191 (2009).
37 Wege, H. A., Kim, S., Paunov, V. N., Zhong, Q. & Velev, O. D. Long-term stabilization of foams and emulsions with in-situ formed microparticles from hydrophobic cellulose. *Langmuir* **24**, 9245-9253 (2008).
38 Frangville, C. *et al.* Fabrication of environmentally biodegradable lignin nanoparticles. *ChemPhysChem* **13**, 4235-4243 (2012).
39 Petridis, L. *et al.* Self-similar multiscale structure of lignin revealed by neutron scattering and molecular dynamics simulation. *Phys. Rev. E: Stat. Nonlinear Soft Matter Phys.* **83**, 061911 (2011).
40 Kim, S., Barraza, H. & Velev, O. D. Intense and selective coloration of foams stabilized with functionalized particles. *J. Mater. Chem.* **19**, 7043-7049 (2009).
41 Langsrud, S., Sundheim, G. & Borgmann-Strahsen, R. Intrinsic and acquired resistance to quaternary ammonium compounds in food-related Pseudomonas spp. *J. Appl. Microbiol.* **95**, 874-882 (2003).
42 Silva, T. *et al.* Particle size, surface charge and concentration dependent ecotoxicity of three organo-coated silver nanoparticles: Comparison between general linear model-predicted and observed toxicity. *Sci. Total Environ.* **468–469**, 968-976 (2014).
43 Tan, S., Erol, M., Attygalle, A., Du, H. & Sukhishvili, S. Synthesis of positively charged silver nanoparticles via photoreduction of $AgNO_3$ in branched polyethyleneimine/HEPES solutions. *Langmuir* **23**, 9836-9843 (2007).
44 Kavlock, R. *et al.* Update on EPA's ToxCast program: Providing high throughput decision support tools for chemical risk management. *Chem. Res. Toxicol.* **25**, 1287-1302 (2012).
45 Choi, O. *et al.* Role of sulfide and ligand strength in controlling nanosilver toxicity. *Water Res.* **43**, 1879-1886 (2009).
46 Wandrey, C., Hernández-Barajas, J. & Hunkeler, D. in *Radical polymerisation polyelectrolytes* Vol. 145 *Advances in Polymer Science* (eds I. Capek *et al.*) Ch. 3, 123-183 (Springer Berlin Heidelberg, 1999).
47 Gélinas, P. & Goulet, J. Neutralization of the activity of eight disinfectants by organic matter. *J. Appl. Bacteriol.* **54**, 243-247 (1983).
48 Lundquist, K., Kirk, T. K. & Connors, W. Fungal degradation of kraft lignin and lignin sulfonates prepared form synthetic 14C-lignins. *Arch. Microbiol.* **112**, 291-296 (1977).
49 Bugg, T. D. H., Ahmad, M., Hardiman, E. M. & Rahmanpour, R. Pathways for degradation of lignin in bacteria and fungi. *Nat. Prod. Rep.* **28**, 1883-1896 (2011).
50 Klein, C. L. *et al.* NM-series of representative manufactured nanomaterials NM-300 silver characterisation, stability, homogeneity. (JRC Scientific and Technical Reports, 2011).